Jupiter's magnetosphere and aurorae observed by the Juno spacecraft during its first polar orbits

Connerney, J. E. P.; Adriani, Alberto; Allegrini, F.; Bagenal, F.; Bolton, S. J.; Bonfond, B.; Cowley, S.W.H.; Gérard, J.C.; Gladstone, G. R.; Grodent, D.

Total number of authors:
22

Published in:
Science

Link to article, DOI:
10.1126/science.aam5928

Publication date:
2017

Document Version
Peer reviewed version

Jupiter's Magnetosphere and Aurorae Observed by the Juno Spacecraft During its First Polar Orbits

Authors: J. E.P. Connerney[1,2], A. Adriani[3], F. Allegrini[4], F. Bagenal[5], S. J. Bolton[4], B. Bonfond[6], S. W. H. Cowley[7], J.-C. Gerard[6], G. R. Gladstone[4], D. Grodent[6], G. Hospodarsky[8], J. L. Jorgensen[9], W. S. Kurth[8], S. M. Levin[10], B. Mauk[11], D. J. McComas[12], A. Mura[3], C. Paranicas[11], E. J. Smith[10], R. M. Thorne[13], P. Valek[4], J. Waite[4]

Affiliations:

[1]Space Research Corporation, Annapolis, MD, 21403, USA.

[2]NASA Goddard Space Flight Center, Greenbelt, MD, 20771, USA.

[3]Institute for Space Astrophysics and Planetology, National Institute for Astrophysics, Rome, 00133, Italy.

[4]Southwest Research Institute, San Antonio, TX, 78238, USA.

[5]Laboratory for Atmospheric and Space Physics, University of Colorado, Boulder, CO, 80303 USA.

[6]Institut d'Astrophysique et de Geophysique, Universite de Liege, Liege, B-4000 Belgium.

[7]University of Leicester, Leicester, LE1 7RH, United Kingdom.

[8]University of Iowa, Iowa City, IA, 52242, USA.

[9]National Space Institute, Technical University of Denmark, Kongens Lyngby, 2800, Denmark.

[10]Jet Propulsion Laboratory, Pasadena, CA, 91109, USA.

[11]Johns Hopkins University, Applied Physics Laboratory, Laurel, MD, 20723.

[12]Department of Astrophysical Sciences, Princeton University, Princeton, NJ, 08544, USA.

[13]Department of Atmospheric and Oceanic Sciences, University of California-Los Angeles, Los Angeles, CA, 90095, USA.

*Correspondence to: jack.connerney@nasa.gov

Abstract: The Juno spacecraft acquired direct observations of the Jovian magnetosphere and auroral emissions from a vantage point above the poles. Juno's capture orbit spanned the Jovian magnetosphere from bow shock to the planet, providing magnetic field, charged particle, and wave phenomena context for Juno's passage over the poles and traverse of Jupiter's hazardous inner radiation belts. Juno's energetic particle and plasma detectors measured electrons precipitating in the polar regions, exciting intense aurorae, observed simultaneously by the ultraviolet and infrared imaging spectrographs. Juno transited beneath the most intense parts of the radiation belts, passed ~4,000 kilometers above the cloudtops at closest approach, well inside the Jovian rings, and recorded the electrical signatures of high velocity impacts with small particles as it traversed the equator.

One Sentence Summary: Juno's instruments provide complete polar maps of Jovian UV aurorae, spatially resolved images of the IR southern aurorae, and in-situ direct measurements of precipitating charged particle populations exciting the aurora.

The Juno Mission serves two principal science objectives. The first is to understand the origin and evolution of Jupiter, informing the formation of our solar system and planetary systems around other stars. Servicing this objective, Juno's measurements of gravity, magnetic fields, and atmospheric composition and circulation probe deep inside Jupiter to constrain its interior structure and composition [1]. The second objective takes advantage of Juno's close-in polar orbits to explore Jupiter's polar magnetosphere and intense aurorae [2]. From a vantage point above the poles, Juno's fields and particles instrumentation gather direct *in-situ* observations of the particle populations exciting the aurora, which are imaged simultaneously by Juno's ultraviolet (UV) and infrared (IR) imaging spectrographs.

Juno's payload includes a suite of fields and particle instruments for in-situ sampling of Jupiter's environment. Juno's magnetometer investigation (MAG) consists of a pair of vector fluxgate magnetometers and proximate star cameras for accurate mapping of the planetary magnetic field [3]. The Jupiter Energetic Particle Detector Instrument (JEDI) measures electrons in the energy range 30 – 800 keV and ions from 10 keV to >1MeV [4] whilst the Jovian Auroral Distributions Experiment (JADE) measures electrons with energies of 0.1 to 100 keV and ions from 5 to 50 keV [5]. Jovian radio and plasma waves are recorded with the Plasma Waves Instrument (Waves) which covers the spectrum from 50 Hz to >40 MHz (*supplementary materials*). Remote observations of the aurora are acquired by a long-slit ultraviolet spectrograph (UVS) counting individual UV photons [6] with wavelengths between 68–210 nm and the Jupiter Infrared Auroral Mapper (JIRAM) which performs imagery and spectrometry over a range (2–5 μm) of infrared wavelengths [7].

Jupiter's dynamo generates the most intense planetary magnetic field in the solar system, with a dipole moment ~20,000 times that of Earth and surface field magnitudes (1 bar level; fluid

planets use a pressure level for reference) about 20 times greater than Earth's [8]. The supersonic solar wind is slowed well upstream of Jupiter forming a bow shock (BS) where the ionized solar wind is abruptly decelerated and heated by the obstruction created by Jupiter's magnetic field. Downstream of the shock lies a region of turbulent flow called the magnetosheath, separated from the region within (the magnetosphere) by the magnetopause (MP). Throughout the magnetosphere, charged particle motion is guided by the magnetic fields originating within Jupiter's interior, and, to a lesser extent, currents distributed throughout the magnetosphere.

Juno encountered the Jovian bow shock just once (June 24, 2016, day of year DOY 176), at a radial distance of 128 R_j (Jovian radii, 1 R_j = 71,492 km), on initial approach to Jupiter (*supplementary material*). Multiple MP crossings were observed spanning the next 5 days (June 25-29, DOY 177-181) at radial distances of 74-114 Rj, prior to orbit insertion on July 4 (DOY 186). Juno's approach and first few orbits lie very nearly in the dawn meridian, so all BS and MP observations are representative of the dawn flank of Jupiter's magnetosphere. Observation of only one bow shock upon approach suggests that the magnetosphere was expanding in size, a conclusion bolstered by the multiple BS encounters experienced outbound (DOY 199-210) during the 53.5 day capture orbit at radial distances of 92–112 Rj before apojove on DOY 213 (~113 Rj), and at distances of 102–108 Rj thereafter (DOY 221-224). Apojove during the 53.5 day orbits occurred at a radial distance of ~113 Rj, so Juno resides at distances of >92 Rj for little more than half of its orbital period (~29 days). Thus on the first two orbits, Juno encountered the MP boundary a great many times at radial distances of ~81–113 Rj.

Juno's traverse through the well-ordered portion of the Jovian magnetosphere is illustrated in Figure 1, in which the measured magnetic field magnitude is compared with a magnetospheric model derived from earlier flybys. The variation in magnetic field magnitude throughout most of

the 10-day interval centered on closest approach to Jupiter (1.06 Rj) at 12:53 UT is well understood based upon prior knowledge of the planetary magnetic field [8] and that of the Jovian magnetodisc [10], a system of azimuthal currents flowing in a washer-shaped disc within a few Rj of the magnetic equator. Upon approach (DOY 235-237), precipitous decreases in the observed magnetic field magnitude result from Juno's traversal of the magnetic equator where magnetodisc currents effectively nullify the internal field. Outbound from perijove (periapsis of Jupiter orbit), Juno traveled through higher magnetic latitudes and did not penetrate the magnetodisc currents so close to Jupiter. Juno's first passage through the Jovian magnetosphere, both inbound and outbound, most closely resembled the inbound portion of the high-latitude Ulysses flyby [11]. These three passages are well described by a magnetodisc model with substantially less current density per unit radius [12] compared to the that prevalent during the Voyager and Pioneer encounters.

The magnetic field observed in the previously unexplored region close to the planet (radius<1.3Rj) was dramatically different from that predicted by existing spherical harmonic models, revealing a planetary magnetic field rich in spatial variation, possibly due to a relatively large dynamo radius [1]. Perhaps the most perplexing observation was one that was missing: the expected magnetic signature of intense field aligned currents (Birkeland currents) associated with the main aurora. We did not identify large magnetic perturbations associated with Juno's traverse of field lines rooted in the main auroral oval (*supplementary material*).

Juno's Waves instrument made observations of radio and plasma wave phenomena throughout the first perijove (Figure 2). These observations were obtained at low altitudes whilst crossing magnetic field lines mapped to Jupiter's complex auroras, so can be compared with terrestrial observations. Jupiter's auroral radio emissions are displayed in Figure 2a, particularly after

perijove. Many of the features in the figure are organized by a fundamental mode of the plasma, the electron cyclotron frequency (simply related to magnetic field intensity by f_{ce}[Hz] = 28|B|[nT]). The radio emissions in Figure 2a-b (and near the top of 2c) are confined to frequencies at or above f_{ce}. These radio emissions are thought to be generated by the cyclotron maser instability (CMI) at frequencies at or just below f_{ce} [13]. Since these radio emissions closely approach the line at f_{ce} in several locations, and show intensification as they do so, it appears that Juno passed very close to (if not through) the source regions for these emissions.

Figures 2c&d show the electric and magnetic components, respectively, of waves at frequencies below 20 kHz. The two intensifications of this emission just after 12:00 and near 13:30 UT demarcate Juno's passage over Jupiter's main auroral oval. These features are thought to be whistler-mode hiss, often called auroral hiss [14] and correspond to features in the energetic electron distributions described below. These waves exist at frequencies below the lower of f_{ce} and f_{pe}, the electron plasma frequency [related to electron density n_e by $n_e = (f_{pe}/8980)^2$ with n_e expressed in cm^{-3} and f_{pe} in Hz]. The lack of features in the wave spectrum identifying the electron plasma frequency makes it difficult to determine the electron density. However, the identification of the emissions in Fig 2c&d below a few 10's of kHz as whistler mode hiss and those above 20 kHz but below f_{ce} in Fig 2b as ordinary mode radio emission (perhaps related to continuum radiation) are both consistent with electron densities of order 10 cm^{-3} in the polar regions. The intensifications in Fig 2c&d with a period of 15 minutes, after 14:00, are suggestive of a link to pulsating auroras reported by Earth-based observers in both ultraviolet and x-ray wavelengths.

The intense burst of noise centered near perijove in Fig 2c and extending into Fig 2b is associated with dust grains impacting the Waves electric antenna (or perhaps the spacecraft). The

grains impact the spacecraft with a relative velocity of >60 km s^{-1}, which provides sufficient kinetic energy to vaporize the grain and a portion of target material, from which a fully-ionized high-temperature gas (~10^5 K) evolves. The expanding plasma cloud from each impact produces an impulse in the electric channel of the Waves receiver that can be counted, yielding an estimated impact rate of a few per second near the jovigraphic equator. These grains are presumably being lost from Jupiter's ring system into the planetary atmosphere.

Electron and ion observations obtained during the same 24-hour interval are presented in Figure 3. The broad bright region between about 4:00 and 8:00 represents a period of time when the spacecraft dipped into Jupiter's radiation belts where high electron and ion intensities are encountered [15]. This period is centered on a local minimum in (dipole) magnetic latitude, at radial distances between 7 and 10 R_j, and ~4 R_j above the magnetic equator. This is close to, but not within, the current-carrying region ($-3<z<3$ R_j) prevailing in magnetodisc models fitted to prior observations confined to lower latitudes. These observations, and intensities encountered near hours 20-22 at radial distances between 9 and 11 Rj, also a local minimum in magnetic latitude but now ~5 R_j below the magnetic equator, suggest a broader distribution of magnetodisc currents about the magnetic equator relative to more distant crossings.

At about 8:35, JEDI and JADE observed localized electron intensification with JEDI electron distributions (Figure 3b) symmetrically aligned with the local magnetic field direction, with the largest intensifications near pitch angles of 0° and 180° [16]. This is the faint feature in Figures 3a,b,d,e just after the broad intensification between 4:00 and 8:00 UT. This occurred when Juno, at a distance of ~6 R_j from Jupiter's center, crossed magnetic field lines that map to the main northern auroral oval. The relatively dark region between ~8:40 and ~12:00 represents the traversal of the polar cap, the region poleward of the northern main auroral oval. That same dark

region is repeated for the southern polar pass, between ~14:00 and ~18:00. Within both of these polar cap regions, JEDI observed mono-directional, upward-directed electron beams confined narrowly to the measured magnetic field directions. Those beams are indicated in Figure 3b by the brightening near 0° pitch angle (8:40 to 11:30) and also near 180° (14:00 to 18:00). Beyond ~18:30 the spacecraft skims a region with magnetic field lines that map to the main auroral oval, where low contrast (low max/min) bi-directional electron beaming is observed. Near the center of Figure 3 (~12:00 to ~13:30), ion and electron sensors responded to additional structures mapping to the main auroral oval and also intense radiation within the high-latitude horns of the radiation belts, shown at higher temporal and spatial resolution in Figure 4. Figure 4a is an energy-time spectrogram for only those electrons moving downward towards Jupiter with pitch angles within +/-15° of the magnetic field. All of the downward energy distributions are monotonic, without peaks in the energy distributions common to Earth auroral distributions. In this brief time span, Juno traversed field lines mapped to the northern auroral oval, the inner radiation belt, and the southern auroral oval.

Figure 4b shows more clearly, on the left, the bi-directional, but asymmetric electron beams observed by the JEDI electron detectors within the northern polar cap. The downward-traveling electron beam (near 180° at left, across the northern polar cap, and near 0° at right, across the southern polar cap) deposits energy into Jupiter's upper atmosphere, potentially powering Jovian auroral emissions. Figure 4c provides an estimate of the energy deposition contributed by 30 – 1000 keV electrons, calculated using electron intensities within 15° of the downward field line (we exclude intensities within the indicated radiation belts, where very high energy electrons penetrate detector shielding).

Energy depositions up to ~80 mW m^{-2} are observed in the northern hemisphere and up to ~200 mW m^{-2} in the southern hemisphere, both observed within the geometric loss cones. These energy depositions are sufficient to account for typical auroral UV luminosities at Jupiter [17]. These measurements imply that Juno may have passed beneath the acceleration region powering Jovian auroral emissions, at least on this occasion.

The highest JEDI energy deposition in the northern hemisphere (near 12:15 UT) was associated with a non-beaming diffuse precipitation, as demonstrated by the character of the pitch angle distribution at that time. While mechanisms for the generation of angular beams with monotonic energy distributions have been discussed in the context of Earth's polar regions [18, 19], the context there may be different, since intense aurora are not generally associated with those beams.

At the center of Figure 4 (~12:45) there appears a localized population of particles (ions or electrons; particle species is unknown, because the JEDI ion sensor is turned off within 10 minutes of periapsis) evidently centered about the actual magnetic equator crossing, in agreement with that computed using spherical harmonic models of the magnetic field (~20° latitude at ~92° sys III longitude). The feature is confined in pitch angle because the loss cones are very large so close to the planet; its origin is unknown.

During the period near closest approach, the JADE ion sensor observed three distinct ion populations (Figure 5). In the northern hemisphere at ~12:13 UT, JADE observed three ion populations, each separated in energy per charge (E/Q) and having a mean energy of ~5, 0.2, and 0.02 keV/Q, respectively. The mean energy of the two higher energy ion populations decreased with time until their abrupt disappearance at ~12:20 UT, coinciding with the spacecraft moving equatorward of the Io (Jupiter's innermost Galilean satellite) flux tube footprint [20]. The TOF

spectra (Figure 5) show strong peaks for mass per charge (m/Q) of 1 (H^+), 8 (O^{++}), 10.67 (S^{+++}), 16 (O^+ or S^{++}), and a weaker peak for 32 (S^+). The strongest signal is from m/q of 16. These ions have energies > 0.1 keV/Q, appear to be moving together, and appear to originate from Io [21,22]. A third, lower energy population of 10's of eV protons is also observed during this timeframe. These low energy protons may be outflowing from Jupiter. During this pass JADE did not detect a significant population of H_3^+ ions. These three distinct ion distributions reappeared in the southern hemisphere starting at ~13:21 as Juno moved poleward of the Io flux tube footprint. The energies and trends seen in these ion distributions are similar to that observed in the northern hemisphere.

The electron distributions showed similar energy dependence as the ions. Starting at 12:10 UT, JADE began to observe ~1 – 10 keV electrons whose energy decreased to below the 0.1 keV lower limit of the sensor by 12:16 as the spacecraft moved towards Jupiter's equator. A similar profile was observed in the southern hemisphere between 13:25 and 13:35. These lower energy electrons are representative of electron distributions in Jupiter's plasma disk (not associated with UV main auroral emissions).

Juno's UV and IR imaging spectrographs captured images and spectra of Jovian northern and southern aurora from a unique vantage point above the poles. The northern auroral oval is offset from the rotation pole by virtue of the geometry of Jupiter's magnetic field, and most longitudes can be imaged from near-equatorial latitudes. Thus many images of the northern aurora have been previously obtained in the IR [23] and UV [24,25] using earth-based and earth-orbiting telescopes (e.g., the Hubble Space Telescope). The southern aurora is more closely confined to high polar latitudes and therefore less visible from near-equatorial latitudes.

Figure 6 displays complete polar maps of Jupiter's northern and southern UV polar aurorae and a polar map of Jupiter's southern aurora in the IR. The UV maps are an assemblage of slit scans across the polar region acquired with every spacecraft rotation (30s). The UVS field of view is steered by spacecraft rotation and the orientation of the UVS scan mirror at the instrument entrance aperture. The UV brightness map is a measure of the energy flux of precipitating electrons that generate auroral emissions. The color ratio quantifies the amount of methane absorption (wavelengths <140 nm) and is a proxy for precipitating electron energy. The more energetic electrons penetrate deeper into the atmosphere before impacting an atmospheric molecule (H_2); UV photons originating deep in the atmosphere suffer more absorption (higher color ratio). Color ratios have long been observed from Earth orbit [26, 27], but with difficulty owing to the geometry of observation.

Jupiter's night-side UV aurora show a very intense and strongly absorbed (high color ratio) patch of outer emissions (at system III longitudes ~230°-280°) in the northern polar region and a complex structure protruding from the main auroral oval into the polar region in the south (system III longitudes ~20°-40°). Substantial brightness and color ratio differences are seen between the hemispheres, attributed to either hemispheric asymmetries [26] or temporal variations.

The IR intensity image of the southern aurora (Figure 6e) is assembled from 25 *L*-band filter images (3.3-3.6 micron). Intensity observed in this band is dominated by multiple H_3^+ emission lines, observed with high signal-to-noise against a background effectively darkened by absorption due to methane [28]. This image was obtained within a span of 12 minutes ~6 hours after perijove. The single pixel spatial resolution is ~150 km. The thickness of the main oval is

quite variable along the arc. The IR aurora is thicker on the dusk side of the planet and thinner on the dawn side, as in UV. The UVS image (Figure 6c) was acquired ~5 hrs prior to the IR image, nearly opposite in local time from the JIRAM image in 6e.

The UV and IR auroral images both show Iogenic emissions [29, 30], either near the instantaneous IFT footprint or along the very long wake left behind the Io footprint, and emissions associated with the other Galilean satellites [31]. The Europa wake is also present (near 120° longitude) in the IR image, partially obscured by main oval emissions. JIRAM can only observe in the plane orthogonal to the spacecraft spin axis. The IR color ratio map (Figure 6f) provides a measure of the temperature of the polar atmosphere at the altitude of the H_3^+ emission. It is compiled from JIRAM spectral observations by taking the ratio of two prominent H_3^+ emission lines (3.5 μm and 3.7 μm). This ratio is dependent upon temperature, ranging from ~1.5 at 850 K to ~1.83 at 1100 K [32]. JIRAM spectra suggest that the polar cap region interior to the main oval between longitudes 30°-90° W is colder than the surrounding area.

Three typical Jovian auroral regions (outer, main, and inner emissions) can be identified in both the UV [25] and IR [33], together with well-identified sub-structures, such as the Io and Ganymede footprints [34], the large regions of UV emission associated with plasma injection signatures [35, 36] and the main emission discontinuity around noon. The overall aurora brightness level is somewhat dim, but not atypically so [37], and the UV color ratio values are similar to previous observations [26, 27]. While there is much similarity between UV and IR auroras, there are differences related to the emission mechanisms at work in both cases. UV emissions are more directly responsive to precipitating particles and as such evidence rapid time variations [37]. In contrast, IR emissions are thermally exited and provide a measurement of upper atmospheric temperature and thereby a measure of energy deposition, whether by particle

precipitation or Joule heating. The IR aurora responds more slowly to energy input [28, 38] and is diagnostic of the transfer of angular momentum from Jupiter to (ionized) mass flowing outward in its magnetosphere [39].

Juno has provided observations of fields and particles in the polar magnetosphere of Jupiter as well as high-resolution images of the auroras at UV and IR wavelengths. While many of the observations have terrestrial analogs it appears that different processes are at work in exciting the aurora and in communicating the ionosphere-magnetosphere interaction. We observed plasmas upwelling from the ionosphere, providing a mechanism whereby Jupiter helps populate its magnetosphere. The weakness of the magnetic field-aligned electric currents associated with the main aurora, and the broadly distributed nature of electron beaming in the polar caps, suggest a radically different conceptual model of Jupiter's interaction with its space environment. The (precipitating) energetic particles associated with Jovian aurora are very different from the peaked energy distributions that power the most intense auroral emissions at Earth.

References and Notes:

[1] Bolton, S. J., Adriani, A., Adumitroaie, V., et al. (2017) Jupiter's interior and deep atmosphere: the first pole-to-pole pass with the Juno spacecraft, *Science*, this issue.

[2] Bagenal, F., Adriani, A., Allegrini, F., et al. (2013) Magnetospheric science objectives of the Juno mission, *Space Sci. Rev.,* 1-69. doi:10.1007/s11214-014-0036-8.

[3] Connerney, J. E. P., Benn, M., Bjarno, et al. (2017) The Juno Magnetic Field Investigation, *Space Sci. Rev.,* doi: 10.1007/s11214-017-0334-z.

[4] Mauk, B.H., Haggerty, D.K., Jaskulek, S.E. et al. (2014) The Jupiter Energetic Particle Detector Instrument (JEDI) Investigation for the Juno Mission, *Space Sci. Rev.,* doi:10.1007/s11214-013-0025-3.

[5] McComas, D.J., Alexander, N., Allegrini, F. et al. (2013) The Jovian Auroral Distributions Experiment (JADE) on the Juno Mission to Jupiter, *Space Sci. Rev*., dos:10.1007/s11214-013-9990-9.

[6] Gladstone, G. R., Persyn, S. C., Eterno, J. S., et al. (2014) The Ultraviolet Spectrograph on NASA's Juno Mission, *Space Sci. Rev.*, doi:10.1007/s11214-014-0040-z.

[7] Adriani A., Filacchione, G., Di Iorio, T. D. , et al. (2014) JIRAM, the Jovian Infrared Auroral Mapper. *Space Sci. Rev.,* doi:10.1007/s11214-014-0094-y.

[8] Connerney, J.E.P. (2015) Planetary magnetism. Volume 10: Planets and Satellites. In G. Schubert and T. Spohn, (Eds.) *Treatise in Geophysics*, Elsevier, Oxford, UK, vol. 10.06, 195-237. ISBN: 978-0-444-63803-1.

[9] Connerney, J. E. P., M. H. Acuña, N. F. Ness, and T. Satoh (1998) New models of Jupiter's magnetic field constrained by the Io flux tube footprint, *J. Geophys. Res.,* 103(A6), 11,929–11,939.

[10] Connerney, J.E.P., Açuna, M.H. & Ness, N.F. (1981) Modeling the Jovian current sheet and inner magnetosphere. *J. Geophys. Res., 86,* 8370 - 8384.

[11] Balogh, A., Dougherty, M. K., Forsyth, R. J., et al., (1992) Magnetic field observations during the Ulysses flyby of Jupiter, *Science* 257, 1515-1518.

[12] The Pioneer 10, Voyager 1, Voyager 2, and outbound leg of the Ulysses flyby were well modeled within 30 Rj of Jupiter using the magnetodisc model cited in reference 9 with a current disc in the magnetic equator having an inner and outer radius of 5 and 50 Rj, respectively; a thickness of +/- 2.5 or 3 Rj, and a current constant of 225. The Ulysses inbound trajectory and Juno's first perijove both required substantially less current (~45% less) and a larger outer radius of the current-carrying magnetodisc (90 Rj).

[13] Treumann, R. A. (2006), The electron-cyclotron maser for astrophysical application, *Astron. Astrophys. Rev.*, 13(4), 229–315, doi:10.1007/s00159-006-0001-y.

[14] Gurnett, D. A., (1966) A Satellite Study of VLF Hiss, *J. Geophys. Res.*, 71, 5599-5615.

[15] de Soria-Santacruz, M., Garrett, H. B., Evans, et al., (2016) An empirical model of the high-energy electron environment at Jupiter, *J. Geophys. Res.*, 121, doi:10.1002/2016JA023059.

[16] Charged particles travel in helical trajectories about the magnetic field. The angle between a particle's velocity vector and the magnetic field direction is referred to as the "pitch angle", which, in a non-uniform magnetic field, varies with the ratio between the perpendicular and parallel components of the particle's velocity. This important quantity determines whether a particle will bounce back and forth, trapped in a non-uniform magnetic field, or, for sufficiently small pitch angles, travel far enough to be absorbed in the atmosphere.

[17] Clarke, J. T. (2012) Auroral Processes on Jupiter and Saturn. In A. Keiling, E. Donovan, F. Bagenal and T. Karlsson (eds.), *Auroral Phenomenology and Magnetospheric Processes: Earth And Other Planets*, American Geophysical Union, Washington, D. C. doi: 10.1029/2011GM001199.

[18] Carlson, C. W. et al., (1998) FAST observations in the downward auroral current region: Energetic upgoing electron beams, parallel potential drops, and ion heating, *Geophys. Res. Lett,* 25, 2017, doi:10.1029/98GL00851.

[19] Mauk, B. H., and J. Saur (2007) Equatorial electron beams and auroral structuring at Jupiter, *J. Geophys. Res.,* 112, A10221, doi:10.1029/2007JA012370.

[20] The Io Flux Tube (IFT) footprint is the area in ionosphere that maps along magnetic field lines to the satellite Io, orbiting in the Jovigraphic equator at ~5.9 Rj radial distance. It is sometimes referred to the "instantaneous" IFT footprint, to distinguish it from the oval traced out in the polar region by the locus of IFT footprints generated as Io moves about Jupiter in system III longitude. The "extended" IFT footprint, or "tail", is the trailing portion of the (instantaneous) footprint.

[21] Kupo, I., Mekler, Y. and Eviatar, A. (1976) Detection of Ionized Sulphur in the Jovian Magnetosphere, *Astrophys. J.* 205, L51-L53.

[22]Thomas, N., F. Bagenal, T. W. Hill, and J. K. Wilson (2004) The Io neutral clouds and plasma torus, in *Jupiter, The Planet, Satellite and Magnetosphere*, eds. F. Bagenal, T. Dowling, and W. McKinnon, vol. 561, Cambrige Univ. Press, Cambridge, U. K.

[23] Stallard, T., Miller, S., Melin, H. (2012) Clues on Ionospheric Electrodynamics from IR Aurora at Jupiter and Saturn. In Auroral Phenomenology and Magnetospheric Processes: Earth and Other Planets. Geophys. Mono. Series, vol. 197, pp. 215–224.

[24] Clarke, J.T., Grodent, D., Cowley, S., et al., (2005) Jupiter's aurorae. In F. Bagenal, T.E. Dowling, and W.B. McKinnon (Eds.), *Jupiter: The planet, satellites, and magnetosphere*, Cambridge University Press, Cambridge, UK.

[25] Grodent, D. (2015) A Brief Review of Ultraviolet Auroral Emissions on Giant Planets *Space Sci Rev* 187: 23. doi:10.1007/s11214-014-0052-8

[26] Gérard J.-C., Grodent, D., Radioti, A., Bonfond, B., Clarke, J. T. (2013) Hubble observations of Jupiter's north–south conjugate ultraviolet aurora. *Icarus* 226, 1559–1567, doi:10.1016/j.icarus.2013.08.017

[27] Gustin, J., Grodent, D., Ray, L. C., et al., (2016) Characteristics of north jovian aurora from STIS FUV spectral images, *Icarus*, 268, 215-241, ISSN 0019-1035, http://dx.doi.org/10.1016/j.icarus.2015.12.048.

[28] Connerney, J.E.P., & Satoh, T. (2000) The H_3+ ion: A remote diagnostic of the Jovian magnetosphere. *Phil. Trans. R. Soc. Lond. A, 358,* 2471 - 2483.

[29] Connerney, J.E.P., Baron, R., Satoh, T., & Owen, T. (1993) Images of excited H_3+ at the Foot of the Io Flux Tube in Jupiter's atmosphere. *Science, 262,* 1035 - 1038.

[30] Clarke, J.T., Ballester, G.E., Trauger, J., et al., (1996) Far-Ultraviolet imaging of Jupiter's aurora and the Io "footprint" with the Hubble Space Telescope Wide Field Planetary Camera 2. *Science, 274,* 404 - 409.

[31] Clarke, J.T., Ajello, J., Ballester, G.E., et al., (2002) Ultraviolet emissions from the magnetic footprints of Io, Ganymede, and Europa on Jupiter. *Nature, 415,* 997 - 1000.

[32] Dinelli, B. M., LeSuer, C. R., Tennyson, J., Amos, R. D., (1995) Ab initio ro-vibrational levels of H_3^+ beyond the Born-Oppenheimer approximation, *Chem. Phys. Lett.*, 232, No. 3, 295-300.

[33] Satoh, T., & Connerney, J.E.P. (1999) Jupiter's H_3+ emissions viewed in corrected Jovimagnetic coordinates. *Icarus, 141,* 236 - 252.

[34] Bonfond, B. (2012) When moons create aurora: The satellite foot-prints on giant planets, in Auroral Phenomenology and Magnetospheric Processes: Earth And Other Planets, edited by A. Keiling et al., pp. 133–140, AGU, Washington, D.C., doi:10.1029/ 2011GM001169.

[35] Mauk, B. H., J. T. Clarke, D. Grodent, J. H. Waite, C. P. Paranicas, and D. J. Williams (2002) Transient aurora on Jupiter from injections of magnetospheric electrons, Nature, 415, 1003–1005.

[36] Bonfond, B., Grodent, B., Gérard, J.-C., et al., (2012) Auroral evidence of Io's control over the magnetosphere of Jupiter, *Geophys. Res. Lett.,* 39, L01105, doi:10.1029/2011GL050253.

[37] Clarke, J. T., et al. (2009) Response of Jupiter's and Saturn's auroral activity to the solar wind, *J. Geophys. Res.*, 114, A05210, doi:10.1029/ 2008JA013694.

[38] Baron, R., Owen, T., Connerney, J.E.P., Satoh, T., & Harrington, J. (1996) Solar wind control of Jupiter's H_3+ aurorae. *Icarus, 120,* 437 - 442.

[39] Hill, T.W. (1979) Inertial limit on corotation. *J. Geophys. Res.* 84, 6554–6558.

[40] Joy, S. P., Kivelson, M. G., Walker, R. J., et al. (2002) Probabilistic models of the Jovian magnetopause and bow shock locations, *J. Geophys. Res.,* 107(A10), 1309, doi:10.1029/2001JA009146.

[41] Dougherty, M. K., Dunlop, M. W., Prange, R., and Rego, D. (1998) Correspondence between field aligned currents observed by Ulysses and HST auroral emission, *Planet. Space Sci.*, 46, No 5, 531-540.

[42] Cowley, S. W. H., Deason, A. J., and Bunce, E. J. (2008) Axi-symmetric models of auroral current systems in Jupiter's magnetosphere with predictions for the Juno mission, *Ann. Geophys.*, 26, 4051-4074, doi:10.5194/angeo-26-4051-2008.

Acknowledgements:

We thank Project and support staff at the Jet Propulsion Laboratory (JPL), Lockheed Martin, and the Southwest Research Institute (SWRI), for the design, implementation, and operation of the Juno spacecraft. We also thank staff at Goddard Space Flight Center, the Applied Physics Laboratory, the University of Iowa, and the Technical University of Denmark, providing science instruments and support. We thank the Italian Space Agency (ASI), B.M Dinelli and F. Fabiano for support of JIRAM. The Belgian contribution to UVS is enabled via support from BELSPO and the ESA-PRODEX program. JPL manages the Juno mission for the principal investigator, Scott Bolton, of SWRI. Supporting data is available in the supplementary material. As agreed with NASA, fully calibrated Juno data is released on schedule via the NASA Planetary Data System at https://pds.nasa.gov/. The Juno mission is funded by NASA and is part of the New Frontiers Program managed at NASA's Marshall Space Flight Center in Huntsville, Alabama.

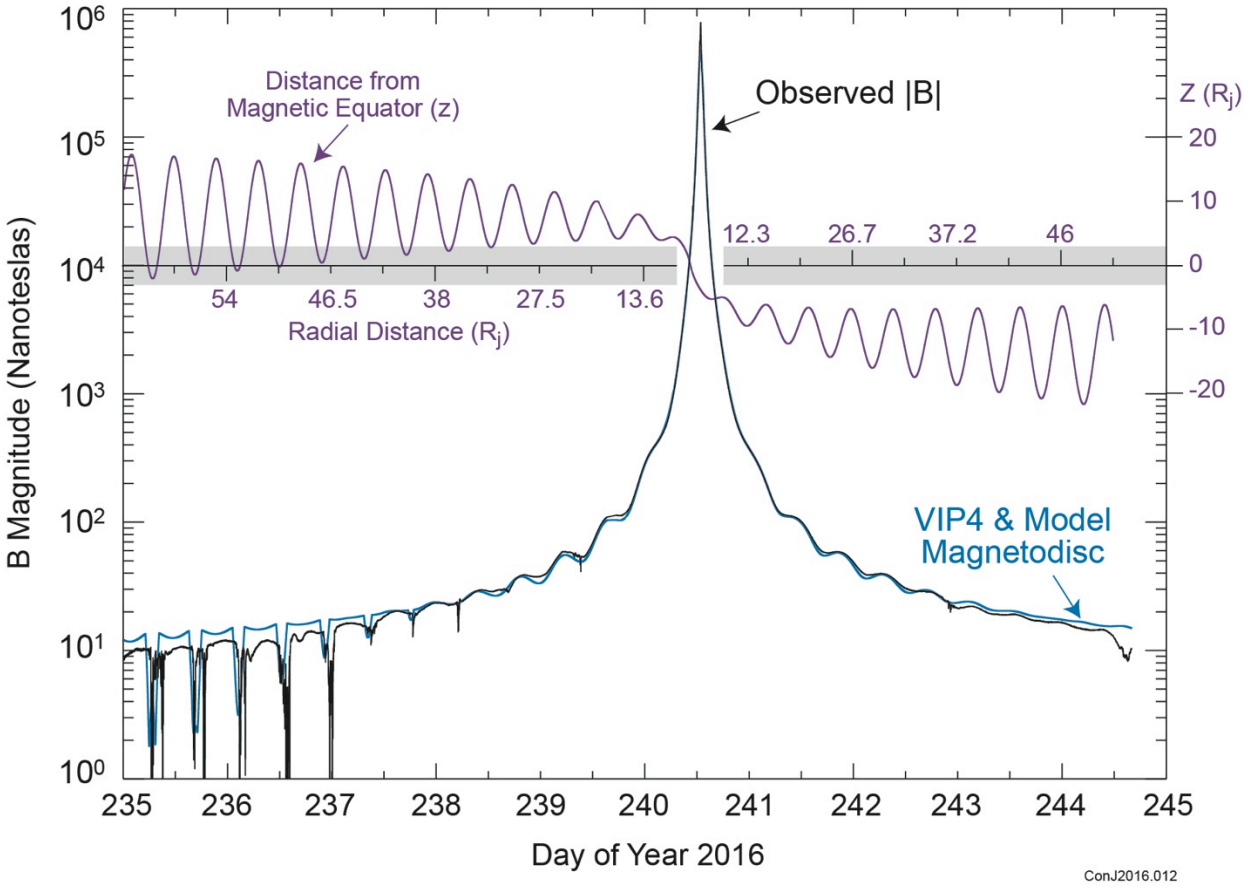

Fig. 1.: Measured magnetic field magnitude (black, solid) and distance above the magnetic equator (purple) as a function of time and distance from Jupiter during Juno's first perijove pass. A model (blue) combines the planetary magnetic field (VIP4 spherical harmonic [9] model) with that of the magnetodisc, a system of azimuthal currents confined to within ~3 Rj of the magnetic

equator (shaded region). The magnetic field magnitude increases by over six orders of magnitude on approach to perijove, where a field of 7.766 G was observed.

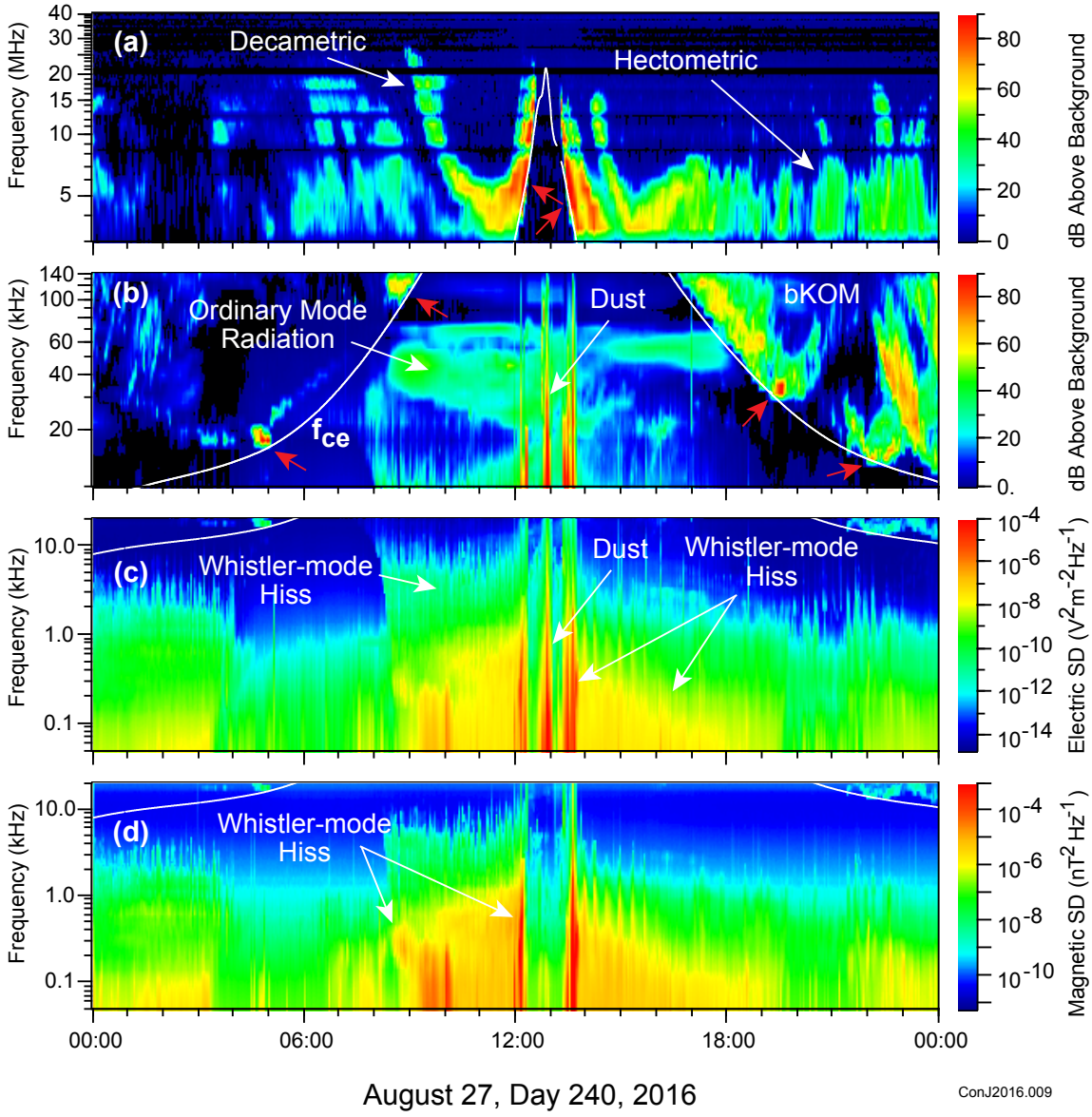

Fig. 2.: Radio and plasma wave observations in Jupiter's polar magnetosphere during Juno's first perijove pass. The intensity or spectral density (SD) of one electric component (panels a-c) of waves as a function of frequency (50 Hz to 40 MHz) and time and one magnetic component (panel d) as a function of frequency (50 Hz to 20 kHz) and time is indicated by the color bar. The white curve in all panels is the electron cyclotron frequency calculated from the magnitude of the magnetic field by $f_{ce}[Hz] = 28|B|[nT]$. Red arrows in panels a and b identify emissions observed with increasing intensity just above f_{ce} that may indicate proximity to or passage through emission source regions.

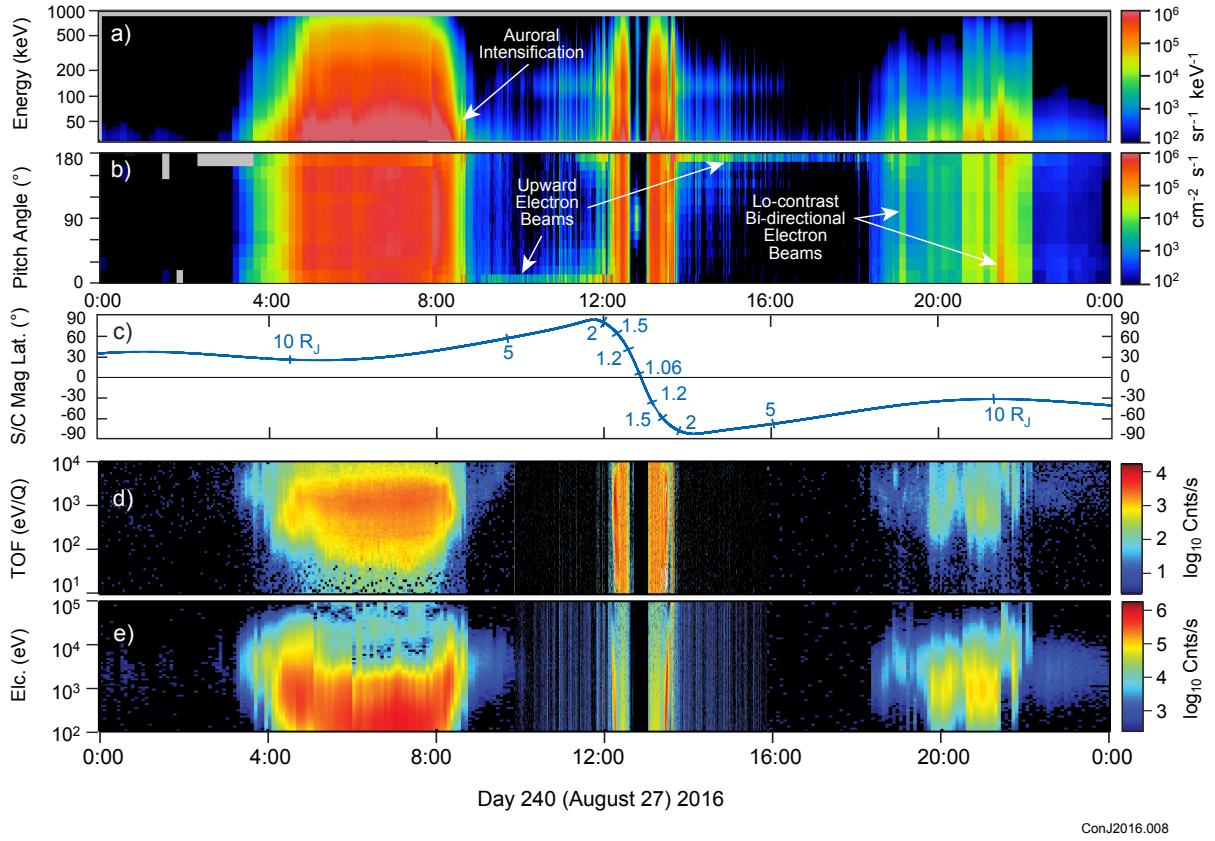

Fig. 3. A 24 hour display, centered on the Juno perijove pass, of energetic electron data from the JEDI instrument in panels (a) and (b) and the lower energy JADE plasma data for ions (panel d) and electrons (panel e). The electron energy spectrogram in panels (a) and (e) sums all angular look directions, whereas the dynamic electron pitch angle spectrogram in panel (b) sums all instrument energy channels. The Juno spacecraft's (dipole) magnetic latitude and radial distance from Jupiter as a function of time is shown in panel (c). In panel (a), from ~9:00 to 16:00 UT, the horizontal band centered on ~150 keV is an artifact caused by intense foreground electrons (energies > 700-800 keV) that fully penetrate JEDI's electron sensor leaving behind a fraction of their actual energy. The JADE ion spectrogram (panel d) sums ion counts over all directions and ion species (units of keV/charge, i.e., E/Q).

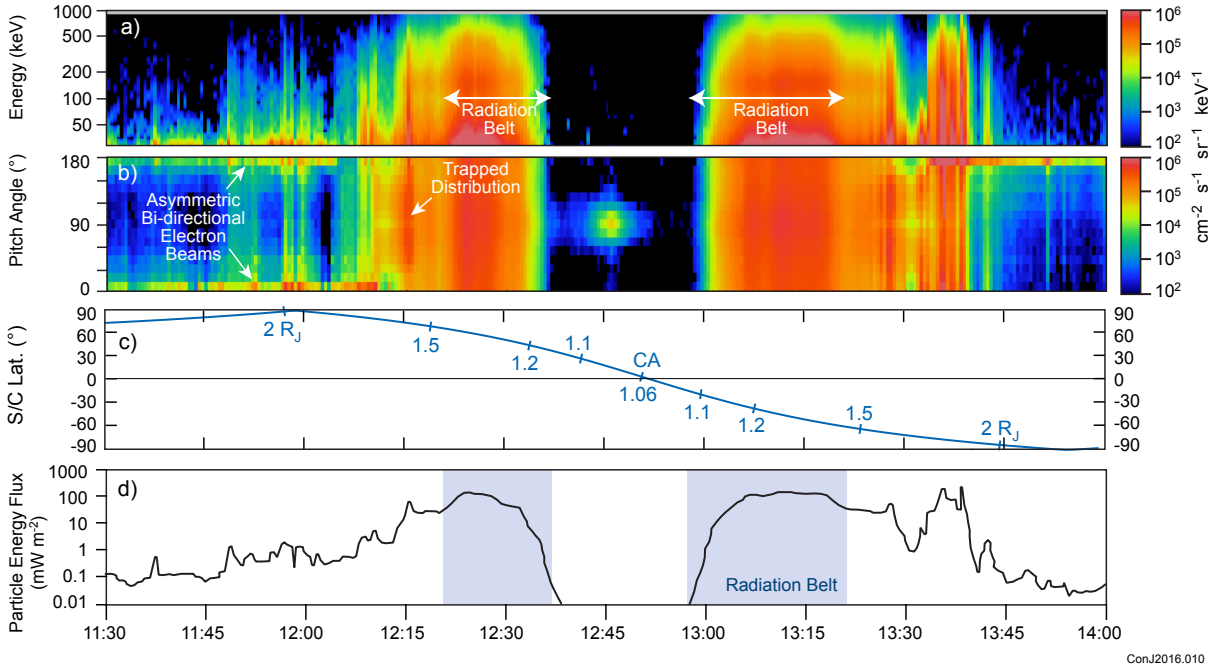

Fig. 4. JEDI electron energy and pitch angles (panels a,b) observed during Juno's polar passages, showing (left) field-aligned, bi-directional, but asymmetric electron beams. These panels are similar to Figure 3a,b, but this energy-time spectrogram (4a) shows only those downward traveling electrons with pitch angles within 15° of the magnetic field. Upward traveling electron beams are in evidence throughout both polar caps. Downward traveling beams (near 180°, left and near 0°, right) can deposit energy into Jupiter's atmosphere, exciting auroral emissions. Panel c shows spacecraft latitude and radial distance. Panel d shows an estimate of the energy deposition from 30 – 1000 keV downward-traveling electrons, using intensities summed over an angle within 15° of the downward field line direction (excluding the radiation belts, where very high-energy electrons penetrate detector shielding).

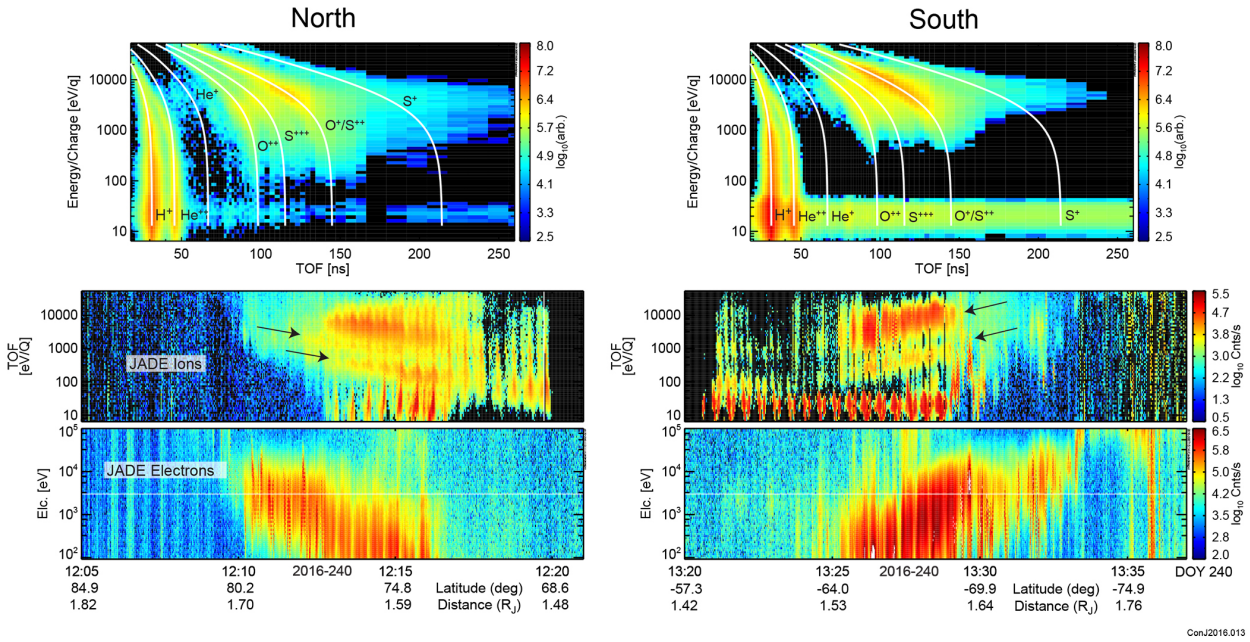

Figure 5: Observations of plasma at latitudes equatorward of the main auroral oval in the northern (left) and southern (right) hemispheres. The top panels show the Energy/Time of Flight (TOF) distributions for the time ranges below. Overlaid on the Energy/TOF plots are traces showing the position of mass/charge (m/q) of 1 (H^+), 2 (H^+ or He^{++}), 4 (He^+), 8 (O^{++}), 10.7 (S^{+++}), 16(O^+ or S^{++}), and 32 (S^+). Due to interactions in the carbon foil of the TOF section, the peak at (m/q)=2 is primarily due to incident protons. Ions (total) as a function of energy and time are shown in the middle panels, and electrons observed by JADE are shown in the bottom panel.

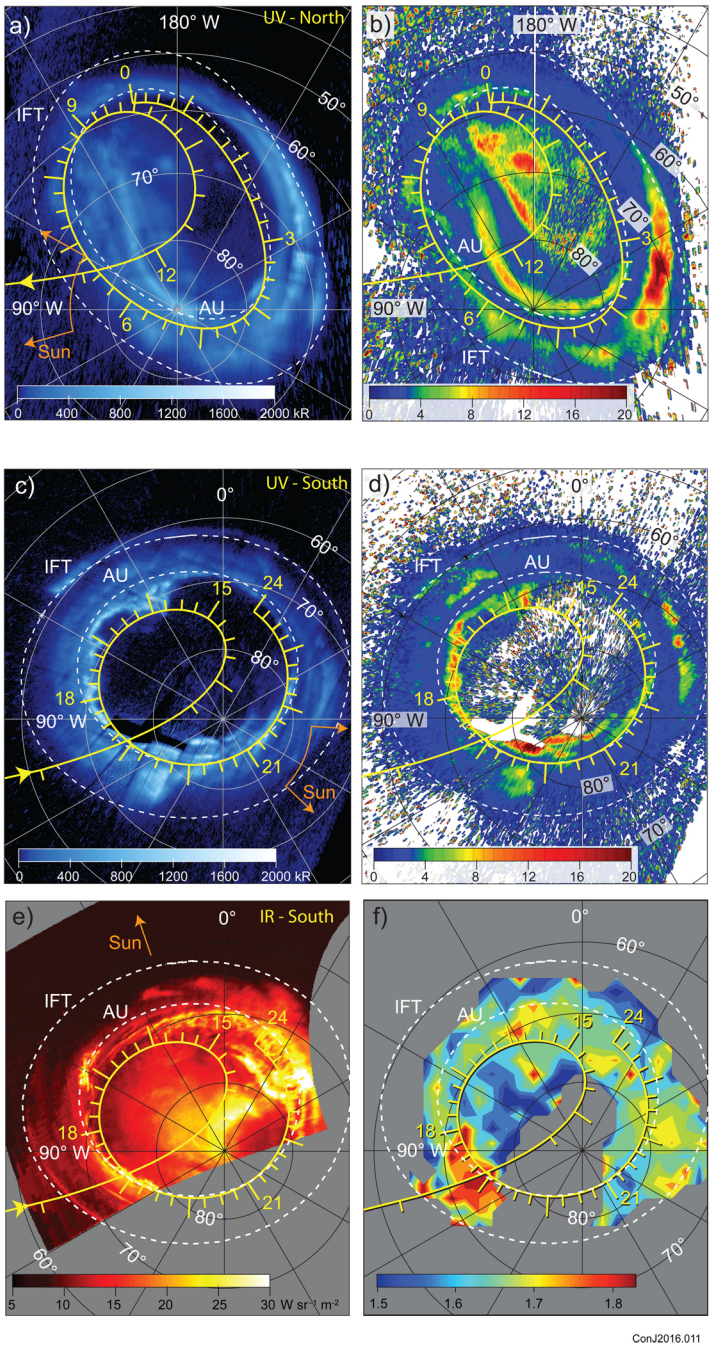

Fig. 6. Orthographic polar projections at the 1 bar level of the ultraviolet (panels a-d) and infrared (e-f) auroral emissions, comparing intensities (left column) and spectral color ratios (right column) with the model auroral oval (AU: innermost dashed oval) and Io fluxtube footprint (IFT: outer dashed circle) computed using the VIP4 model internal field [9] and model magnetodisc. The footprint of the spacecraft is shown by the solid line, with hourly tic marks to facilitate comparison with in-situ fields and particles observations shown in Figures 1-4. Top panels are northern UV aurora, center and bottom panels compare UV and IR southern aurora. UV intensities are summed between 60-180 nm and UV color ratios are given as 155-162nm/123-130nm. UVS north (south) polar data acquired between 09:52:35 and 10:40:59

(13:22:39 and 14:34:12) UT on DOY 240, 2016. The infrared aurora (left) is a mosaic of 25 *L* band filter images (3.3-3.6 um) obtained with 1s integration time from between 18:09:21 and 18:22:10 UT on DOY 240, showing emission due to the H_3^+ ion. The spectral color ratio (right) is obtained from JIRAM spectra acquired between 14:45 and 19:51 UT as the ratio of two H_3^+ emission lines (3.5 μm/3.7 μm) that is diagnostic of temperature (blue relatively cold, red, hot). Gray regions are areas devoid of data.

Supplementary Materials for

Jupiter's Magnetosphere and Aurorae Observed by the Juno Spacecraft During its First Polar Orbits

J. E.P. Connerney[1,2], A. Adriani[3], F. Allegrini[4], F. Bagenal[5], S. J. Bolton[4], B. Bonfond[6], S. W. H. Cowley[7], J.-C. Gerard[6], G. R. Gladstone[4], D. Grodent[6], G. Hospodarsky[8], J. Jorgensen[9], W. S. Kurth[8], S. M. Levin[10], B. Mauk[11], D. J. McComas[12], A. Mura[3], C. Paranicas[11], E. J. Smith[10], R. M. Thorne[13], P. Valek[4], J. Waite[4]

correspondence to: jack.connerney@nasa.gov

This PDF file includes:

Materials and Methods
Supplementary Text
Figs. S1 to S4
References *(39-40)*

Materials and Methods

Waves Investigation

The Waves instrument utilizes two sensors: i) an electric dipole antenna mounted on the aft flight deck, oriented with its sensitive axis parallel to Juno's y axis and ii) a search coil magnetometer mounted to the spacecraft with its sensitive axis parallel to Juno's z axis (the spacecraft rotation axis). Search coil output is processed by the Low Frequency Receiver over a frequency range of 50 Hz to 20 kHz. Electric field signals are processed via an identical channel. Waveforms from these channels are Fourier transformed to produce a logarithmically-spaced spectrum with ~16 channels per decade. A mid-frequency band included in the Low Frequency Receiver processes electric dipole signals from 10 kHz to 150 kHz. These waveforms are Fourier transformed to produce a logarithmically-spaced spectrum with ~15 channels per decade. Redundant High Frequency Receivers process electric dipole signals between 100 kHz and 40 MHz. This receiver includes channels from 3 to 40 MHz (with 1 MHz bandwidth) in which amplitudes are detected in a sweep frequency receiver mode. Between 100 kHz and 3 MHz, waveforms are acquired and processed to generate a logarithmically-spaced spectrum with ~18 channels per decade. All of these spectral components can be collected every 1, 10, or 30 seconds, with the selection dependent on telemetry allocation. Waveforms from each of these receivers may be collected in high-speed burst modes, for limited intervals of time at low duty cycle. A 1-MHz band tuned to include the local electron cyclotron frequency is also used for burst waveforms from the High Frequency Receiver.

Supplementary Text

Bow Shock and Magnetopause Observations

During the approach to Jupiter, Juno encountered the Jovian bow shock (BS) just once at 18:16 UT on 24 June 2016 (DOY 176) at a radial distance of ~128 Jovian radii. All times are spacecraft event times (SCET) – universal time (UT). Figure S1 shows observations of ions observed by JADE, electric fields observed by Waves, and the magnetic field observed by the MAG instrument. Prior to crossing the shock, the JADE Ion instrument observed two well-defined peaks in energy per charge for cold protons and alpha particles as is usual for the solar wind. Waves observed electron plasma oscillations at frequencies of ~7 kHz, indicating an electron density of about 0.6 cm^{-3}. The magnetic field magnitude was about 1.5 nT. The shock itself is characterized by heating of the plasma as indicated by the much broader energy distribution in the JADE data. The Waves data show a broadband burst of waves and a cessation of the upstream plasma oscillations. The magnetic field magnitude increases to about 5 nT indicating a

relatively strong shock, even though Juno is near the dawn meridian at a magnetic local time of 6.3 h.

The first magnetopause crossing (MP) occurred at ~21:20 UT on 25 June 2016 (DOY177) at ~114 R_J. Figure S2 shows JADE, Waves, and MAG data for this event. The dashed line indicates the MP. Both the electrons and ions observed by JADE show much more energetic particle populations just inside the magnetopause with evidence of further energization as Juno continued inward. The magnetopause is clearly observed in the Waves electric field spectrum with the appearance of trapped continuum radiation that fills the magnetospheric cavity. There is an ordinary mode emission that propagates down to the electron plasma frequency; hence, the low-frequency cutoff provides information on the magnetospheric density. Just inside the MP, the density is about 0.005 cm^{-3}. The magnetic field shows a strong rotation at the MP, but is highly variable during this time. A partial MP crossing is also evident in Figure S2 at about 20:21. This is seen primarily in the JADE and MAG data. Additional MP crossings were observed on DOY 180 and 181 at radial distances of 84-74 R_J as shown in Figure S3.

Juno's approach lies very nearly in the dawn meridian, so all BS and MP observations are representative of the dawn flank of Jupiter's magnetosphere (Figure S3). Observation of one BS and initially only one MP upon approach suggests that Juno encountered a magnetosphere expanding in size. The multiple MP crossings detected 4 days later at 84 to 74 R_J suggests a contracting magnetosphere as Juno approached its orbit insertion on DOY 186.

Search for Birkeland Currents Crossing the Main Aurora

Figures S4 shows magnetic field perturbations and electron intensities observed as Juno crossed magnetic field lines rooted in the main auroral oval. In order to see small fluctuations in the magnetic field in the presence of a large background field, we fit a spline function to each component of the vector magnetic field in planetocentric spherical coordinates and show here the difference between the observed field and the spline fit. The differences are averaged with a 30 s running average (s/c spin period) to remove residual artifacts associated with the coordinate transformation to an inertial system. Figure S4 shows the period associated (main text) with crossing the main auroral oval inbound (DOY 240 08:15 to 09:00) at ~6 R_j radial distance. During this inbound crossing, Birkeland currents may have contributed only a few nT as Juno transited the main auroral oval (against a background field of ~2500 nT to ~4000 nT). This is much less than that observed (~20 nT) by the Ulysses spacecraft [41] in transit of the main auroral oval at greater radial distances (15-20 R_j). One expects Birkeland current densities to increase dramatically with decreasing distance to Jupiter [42].

Spacecraft attitude reconstruction (for elements on the MAG boom) has not been completed, so estimates of the magnitude of fluctuations associated with Birkeland currents in much stronger fields are not available at this time.

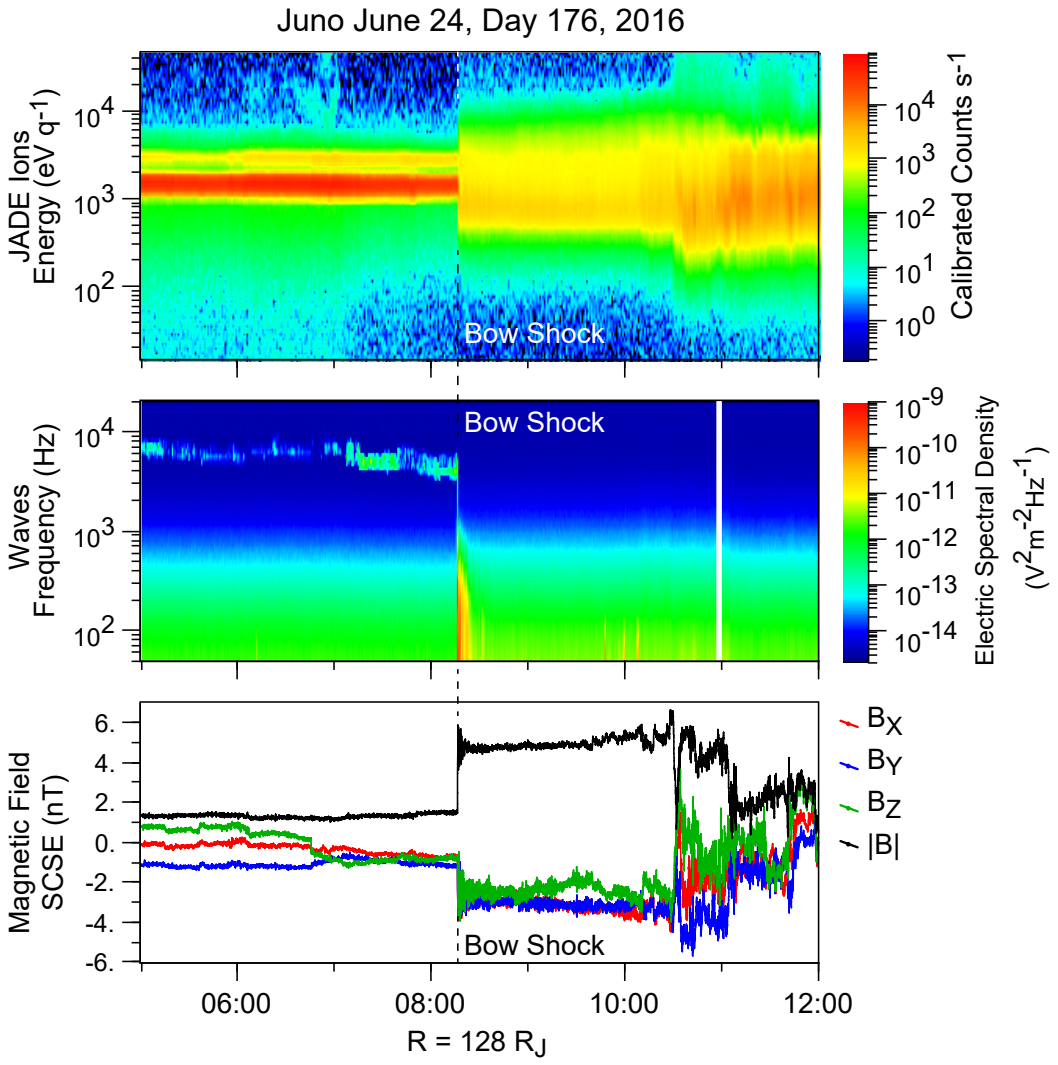

Fig. S1.

Bow shock observations. (A) Ions (primarily protons and alpha particles) energy (eV/q) and count rate as a function of time, (B) electric field spectral density (white vertical line is a data gap), and (C) magnetic field components in the SCSE coordinate system during Juno's passage through the bow shock. In the SCSE coordinate system, x is aligned with the sun-spacecraft vector, y is parallel to the sun's equator, and z completes the right-handed system. At the time of observation Juno was 128 R_j distant.

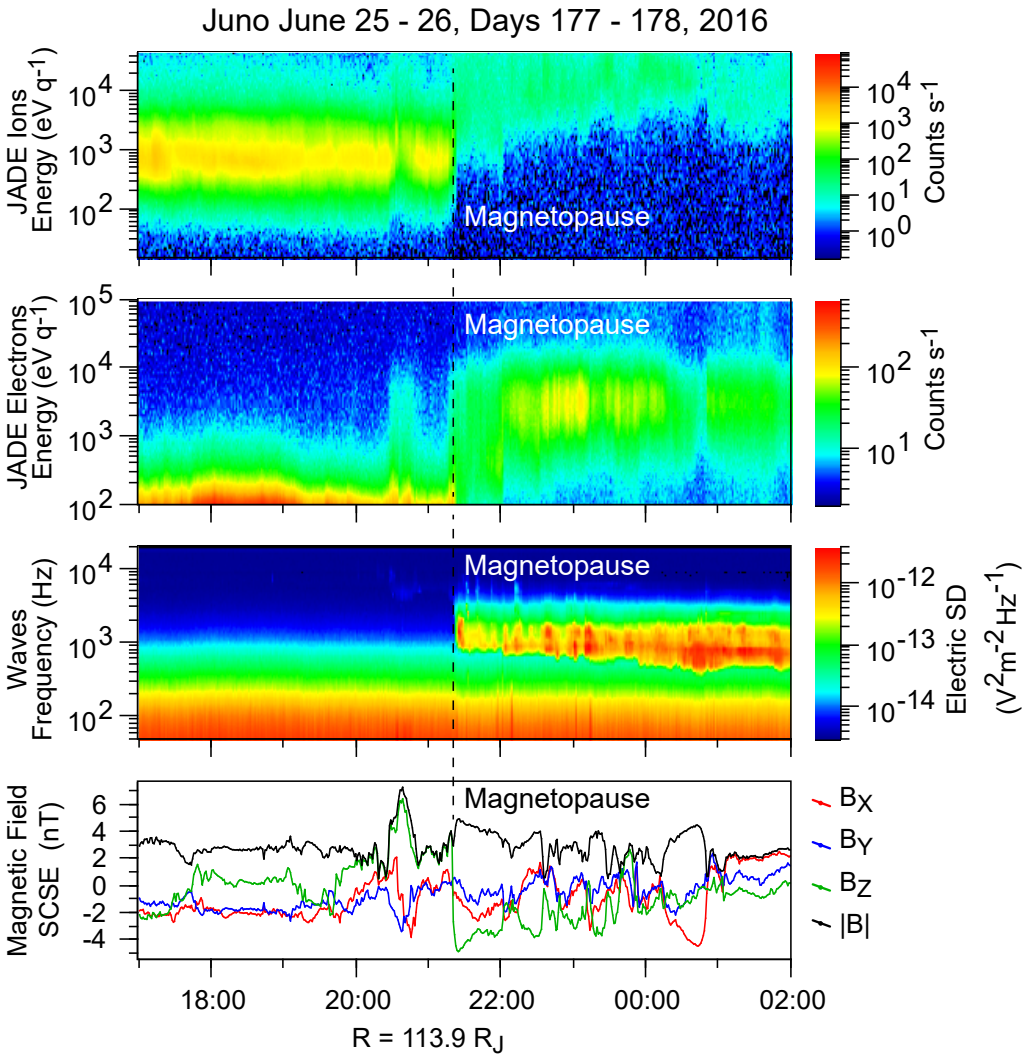

Fig. S2

Magnetopause observations. (A) ions as in figure S1, (B) energy (eV/q) and count rate of electrons, (C) electric field spectral density and (D) magnetic field components as in Figure S1 during Juno's entry into the Jovian magnetosphere prior to orbit insertion. At the time of observation Juno was 113.9 R_j distant.

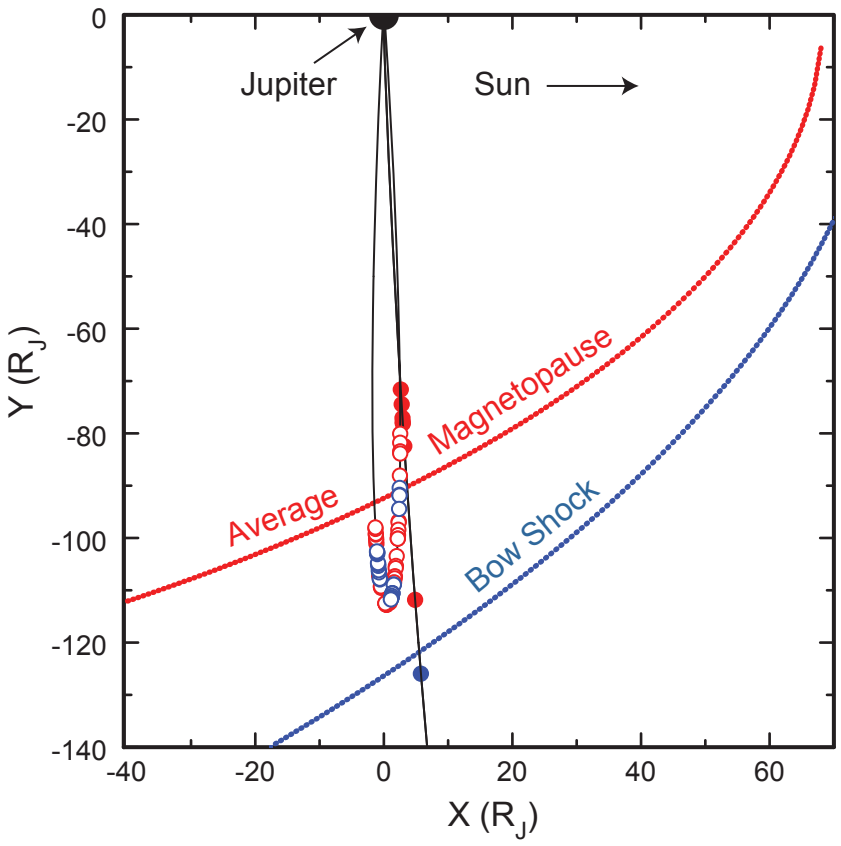

Fig. S3

Locations of the bow shock (blue) and magnetopause (red) boundaries encountered inbound prior to Jupiter orbit insertion (filled) and during the first orbit (open) compared with the average positions fitted to prior encounters [40]. Position is given in Jupiter Solar Orbit (JSO) coordinates where X is directed from Jupiter to the Sun, Y is in Jupiter's orbital plane and nearly opposite to the orbital velocity, and Z completes the orthogonal system.

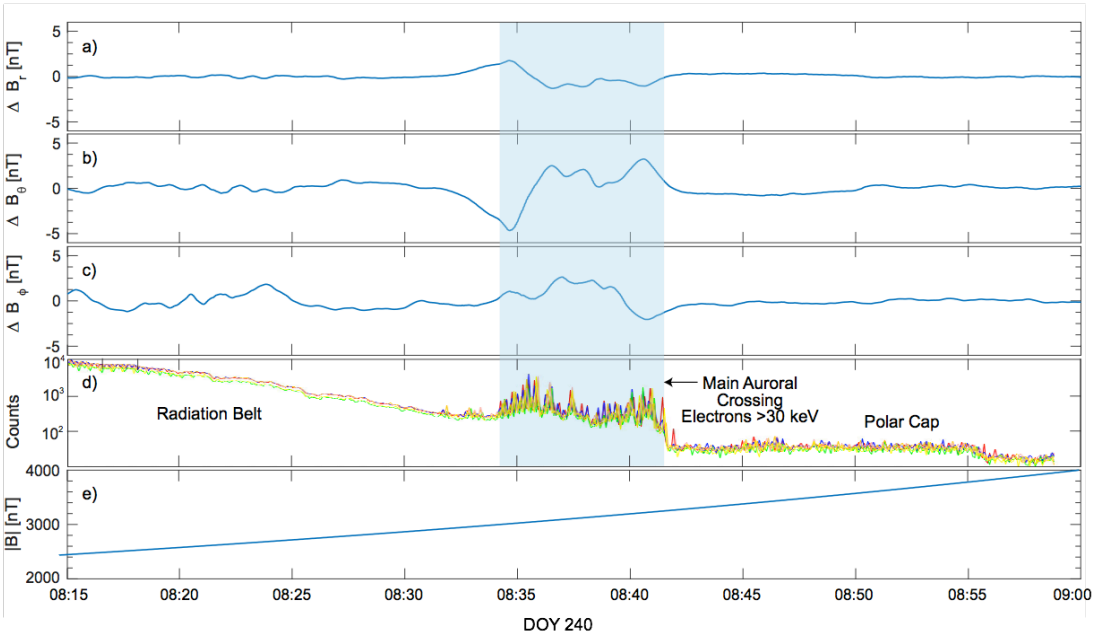

Fig. S4

Magnetic fluctuations observed during Juno's traversal of the main auroral oval (shaded region) at ~08:35 DOY 240. (A, B, C) the radial, theta, and phi components of the perturbation magnetic field (after background subtraction). (E) the magnitude of the magnetic field before background subtraction. (D) the measured intensities of electrons with energies greater than 30 keV as counted by JEDI's 6 solid-state detectors. The magnitude of the spin modulation shows that these electrons are confined to a narrow beam.